

Facile Protection of Lithium Metal for All-Solid-State Batteries

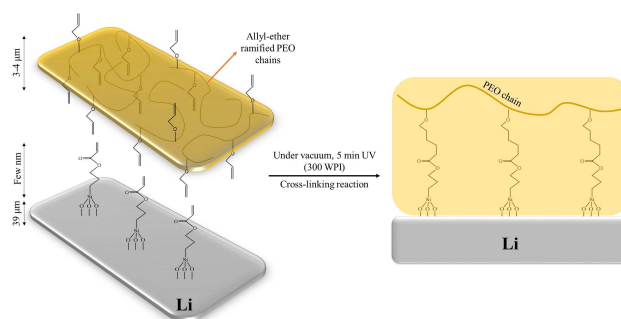
Nicolas Delaporte,^[a] Abdelbast Guerfi,^[a] Hendrix Demers,^[a] Henning Lorrmann,^[b] Andrea Paoella,^{*[a]} and Karim Zaghib^{*[a]}

A nanolayer of reactive propyl acrylate silane groups was deposited on a lithium surface by using a simple dipping method. The polymerization of cross-linkable silane groups with a layer of ally-ether-ramified polyethylene oxide was induced by UV light. SEM analysis revealed a good dispersion of silane groups grafted on the lithium surface and a layer of polymer of about 4 μm was obtained after casting and reticulation. The electrochemical performance for the unmodified and modified lithium electrodes were compared in symmetrical Li/LLZO/Li cells. Stable plating/stripping and low interfacial resistance were obtained when the modified lithium was utilized, indicating that the combination of silane and polymer deposition is promising to increase Li-metal/garnet contact.

Lithium-ion batteries are a promising energy storage technology. The demand for high energy storage in commercial devices and EVs requires the use of lithium metal anodes. Unfortunately, the standard carbonate-based liquid electrolyte presents a safety risk due to high flammability of the solvent. Lithium metal can easily form dendrites that cause short circuit in liquid electrolyte.^[1,2] Solid electrolytes can serve as a physical barrier, and several options were considered: a polymer^[3] like polyethylene oxide (PEO):LiTFSI blend, ceramics such as garnet^[4] and Nasicon,^[5] and hybrid ceramic polymer electrolyte.^[6] Garnet lithium lanthanum zirconate $\text{Li}_7\text{La}_3\text{Zr}_2\text{O}_{12}$ (LLZO) is a promising candidate as solid electrolyte due to its high structural stability at high voltage (up to 5 V) and good ionic conductivity (around 0.5 mS cm^{-1}). The high resistance between LLZO and lithium metal is a serious issue that must be addressed in order to develop an all-solid battery. In addition, the conversion of cubic LLZO to poorly conductive tetragonal LLZO occurs at the lithium metal interface, as reported by Ma *et al.*^[7] Actually, several physical and chemical methods were proposed to improve the contact between LLZO and lithium metal: PEO gel,^[8]

aluminum^[9] and silicon deposition. In this work, we propose a new large-scale method to protect lithium metal via silane deposition combined with polymer casting and reticulation to improve its contact with the LLZO pellet. Porcarelli *et al.* report the UV-induced (co)polymerization of PEO with tetraglyme at various lithium salt concentrations.^[10] In our work, we induced a UV polymerization by using a silane-modified lithium with cross-linkable groups and Ally-ether ramified PEO. We decided to use silane because of its good interaction with lithium metal as previously reported.^[11,12]

PEO-LiTFSI is well known solution as solid polymer electrolyte as reported by Armand.^[13] Nakayama *et al.* proposed the addition of the plasticizers poly(ethylene glycol) (PEG)-borate ester and the final battery Li/boron-PEO/LiFePO₄ delivered stable charge/discharge cycles (> 150 cycles) at 30 °C.^[14] A recent approach proposed by Goodenough and co-workers consisted of adding a cross-linked polymer between garnet and lithium metal to improve their contact and delivered stable electrochemical cycling performance.^[8] Inspired by their work, Scheme 1 illustrates a procedure to reduce the Li-metal/bare-garnet interfacial resistance by a simple dipping method to form nanolayers of propyl acrylate silane groups on the lithium surface. Then, a thin layer (~4 μm) of Ally-ether ramified PEO containing a lithium salt and a photoinitiator was casted on its surface. After the cross-linking reaction under UV light, a strong link between the lithium and the polymer layer was obtained. This method is versatile and can be extended to other kind of cross-linkable polymers with acrylate or epoxy functions and other type of silane with mercapto or allyl ether end groups, for instance. Finally, our method is appealing because easily adapted to a large-scale process, in contrast to Atomic Layer



Scheme 1. Schematic representation of Li metal surface modified by a thin layer of reactive propyl acrylate silane groups on which a thin (ca. 4 μm) layer of ally-ether-ramified PEO + LiTFSI salt is deposited. A strong contact between the lithium surface and polymer is obtained after reticulation under UV light.

[a] Dr. N. Delaporte, Dr. A. Guerfi, Dr. H. Demers, Dr. A. Paoella, Dr. K. Zaghib
Center of Excellence in Transportation
Electrification and Energy Storage
1806, boul. Lionel-Boulet, Varennes, QC, J3X 1S1, Canada
E-mail: Paoella.Andrea2@hydro.qc.ca
Zaghib.Karim@hydro.qc.ca

[b] Dr. H. Lorrmann
Fraunhofer-Institut für Siliciumforschung ISC
Neunerplatz 2 97082 Würzburg, Germany

© 2019 The Authors. Published by Wiley-VCH Verlag GmbH & Co. KGaA. This is an open access article under the terms of the Creative Commons Attribution Non-Commercial NoDerivs License, which permits use and distribution in any medium, provided the original work is properly cited, the use is non-commercial and no modifications or adaptations are made.

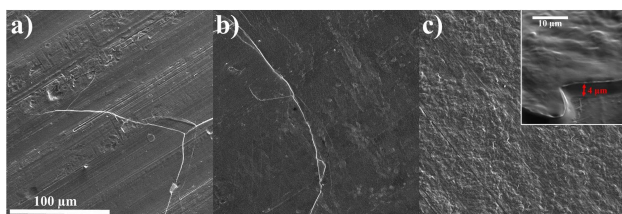


Figure 1. SEM images of a) unmodified lithium, b) lithium@silane, and c) lithium@silane with PEO coating. The insert shows the PEO layer of about 4 μm thick on lithium surface.

Deposition (ALD) already used for the surface modification of garnet with Au,^[15] Ge^[16] or ZnO^[17] coatings.

Unmodified and treated lithium surfaces were analyzed using scanning electron microscopy (SEM). Figure 1 shows the SEM images of a) unmodified lithium, b) lithium@silane and c) lithium@silane with PEO coating. The straight lines observed at the surface of fresh lithium (see Figure 1a) disappeared after reaction with propyl acrylate silane groups (see Figure 1b) confirming that a uniform coverage of few nm was obtained. The layer of PEO casted on lithium@silane is well observed by SEM (Figure 1c) and its thickness was estimated around 4 μm as put in evidence by the magnification in insert of Figure 1.

The effect of surface modification of lithium foil was examined using Li-metal/LLZO/Li-metal symmetric cells. Electrochemical impedance spectroscopy (EIS) was used to measure the interfacial resistance between modified or fresh lithium electrodes and the garnet electrolyte. Figure 2 shows the Nyquist plots obtained at 25 (Figure 2a) and 80 °C (Figure 2b) for unmodified lithium (■), lithium with PEO coating (●) and lithium@silane with PEO coating (▲). The Li-metal/LLZO/Li-metal cell (■) at 25 °C showed an obvious semicircle at high frequency (see insert in Figure 2a) that indicates a large resistance of about 550 k Ω , which is mainly attributed to the poor contact between the Li metal and the bare-garnet pellet. In fact, the garnet-structure $\text{Li}_7\text{La}_3\text{Zr}_2\text{O}_{12}$ is characterized by high Li-ion conductivity (0.1–1 mS cm^{-1}),^[18] suggesting that the rate-controlling step is not in the bulk of the solid electrolyte, but at

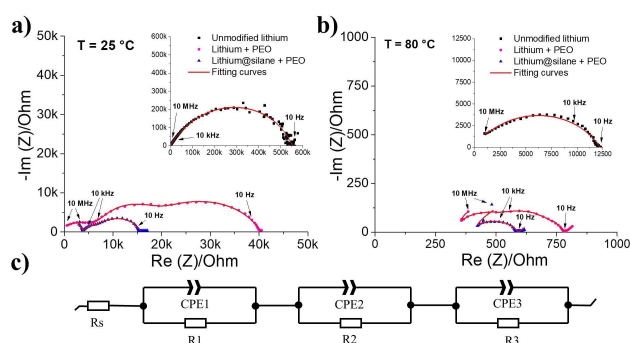


Figure 2. Electrochemical impedance spectroscopy measurements recorded at a) 25 °C and b) 80 °C for Li/LLZO/Li symmetric cells assembled with: unmodified lithium (■), lithium with PEO coating (●), and lithium@silane with PEO coating (▲). The inserts show the Nyquist plot when unmodified lithium (■) is used. C) Equivalent circuit used for modeling the EIS data represented by the red lines (—).

the interface between the electrode and the electrolyte material.^[19] EIS data were modeled using an equivalent circuit shown in Figure 2c. Generally, a similar model is employed to depict the Li/LLZO/Li cells behavior^[20] and is characterized by a succession of constant phase elements (CPE) and resistances related to the LLZO bulk, grain boundary and Li-LLZO interface.^[21,22] Semicircles at high frequencies are attributable to the total resistance of the LLZO pellet and the low frequency semi-circles can be assigned to the interfacial resistance.^[23] After PEO coating on lithium surface (lithium+PEO (●)), the impedance has drastically diminished and in particular the resistance at the lithium-LLZO interface (low frequencies). Finally, the combination of both the silane and polymer layers (lithium@silane+PEO (▲)) led to a total resistance of ~ 12 k Ω at 25 °C, very near of that obtained for unmodified lithium at 80 °C (see insert in Figure 2b). This decrease in interfacial resistance is undoubtedly attributed to the greatly enhanced contact after lithium modification.

The voltage profiles for the Li/LLZO/Li symmetric cells at 80 °C are presented in Figure 3, and the results are in agreement with the decreased interfacial resistance observed after surface modification of lithium. The cell assembled with fresh lithium (—) has higher voltage hysteresis for each cycling current and short-circuited after less than 130 h of cycling. In contrast, the voltage profiles for modified-Li/LLZO/modified-Li cells showed smaller voltage hysteresis of about 80 and 50 mV at 0.1 mA cm^{-2} when lithium with PEO coating (—) and lithium@silane with PEO coating (—) were used, respectively. These cells were characterized by a long-term stable electrochemical stripping/plating process (see Figure 3b). Moreover, the last one (—) displayed flat voltage plateaus during both plating and stripping. In conclusion, our work shows a new and scalable method to reduce the interfacial resistance between lithium metal and electrolyte ceramics. The symmetrical cells Li/silane-PEO/LLZO/silane-PEO/Li showed stable plating/stripping, indicating that the combination of silane and polymer deposition is promising for increasing the Li-metal/garnet contact.

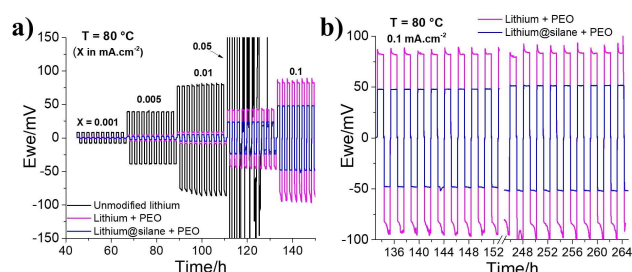


Figure 3. a) Galvanostatic stripping-plating cycling at 80 °C at different current densities for Li/LLZO/Li symmetric cells assembled with: unmodified lithium (—), lithium with PEO coating (—) and lithium@silane with PEO coating (—). b) Long-term galvanostatic cycling at 0.1 mA cm^{-2} for cells assembled with modified lithium electrodes.

Experimental Section

Preparation of Polymer Solution

Allyl-ether-ramified polyethylene oxide (provided by Hydro-Québec) was dispersed in a small amount of anhydrous tetrahydrofuran (THF from Sigma-Aldrich) that was mixed until a viscous solution was obtained. Lithium bis(trifluoromethanesulfonyl)imide salt (LiTFSI from Sigma-Aldrich) corresponding to a O:Li molar ratio of 20:1 was then added to the polymer solution. After mixing for several hours, the polymer solution was diluted with THF to obtain 26.8 wt.% of solid (polymer and salt). Finally, 0.4 wt.% of Omnirad 651 photoinitiator (from IGM resins) was dispersed in the polymer solution, and then the mixture was stored in the dark.

Surface Modification of Lithium Foil with 3-(Trimethoxysilyl)propyl Acrylate

One side of a lithium foil (39 μm thick, provided by Hydro-Québec) was reacted for 2 minutes with 0.25 mL cm^{-2} of a 10^{-1} M 3-(Trimethoxysilyl)propyl acrylate in THF solution under a fume hood in a dry-room chamber. After the solvent was evaporated, the lithium foil was rinsed two times with fresh THF and placed under vacuum for at least 15 h.

Polymer Casting on Lithium Foil

The diluted polymer solution was first spread on a polypropylene (PP) sheet to estimate the thickness of the deposited film after drying and reticulation. Wet polymer casting corresponding to 1 mil (~ 25 μm), 2 mils (~ 50 μm) and 3 mils (~ 75 μm) produced dry films of about 3–4, 6 and 9 μm thickness, respectively. The fresh and silane-modified lithium foils (18 $\text{cm} \times 4.5$ cm) were then coated with the polymer solution (~ 20 μm wet) and directly placed in an oven at 50 °C for 10 minutes. Subsequently, the lithium foils were introduced in a Büchner glass assembly and put under continuous vacuum for 2 minutes followed by exposure to UV light (300 WPI) at a distance of 50 cm for 5 minutes. After crosslinking, the lithium was kept under vacuum in an oven at 80 °C for at least 15 h before utilization.

Surface Morphology of Lithium Foil

Li metal surfaces were analyzed using scanning electron microscope (SEM) Lyra 3 by TESCAN. Samples were prepared in a dry chamber and inserted in the SEM using an air-tight transfer holder to minimize external contamination. The micrograph and X-ray map were acquired at an accelerating voltage of 5 kV, a probe current of 500 pA and a working distance of 9 mm.

Synthesis and Densification of LLZO Pellets

Ga-doped LLZO was synthesized following a solid-state method.^[24] The LLZO pellets were prepared by annealing 1-mm thick pellets at 1100 °C for 16 h in an alumina crucible surrounded by sacrificial powder of LLZO. The final pellets were polished in a glove box.

Electrochemical Characterization

Unmodified or modified lithium electrodes (10-mm diameter) were hot-pressed on each side of a LLZO pellet (13-mm diameter) at 80 °C under vacuum for 3 min. The components were assembled in a coin cell in a glove box filled with argon ($\text{O}_2 < 10$ ppm, $\text{H}_2\text{O} <$

10 ppm). The coin cells were electrochemically characterized with a BioLogic VMP3 potentiostat.

Electrochemical impedance measurements of the cells were performed at 25 and 80 °C with an AC amplitude of 10 mV and a frequency range of 10 MHz to 10 mHz. Galvanostatic stripping-plating cycling of the symmetric cells was recorded at 80 °C with different current densities ranging from 0.001 to 0.1 mA cm^{-2} .

Acknowledgements

This research was financially supported by HydroQuebec and Ministry of Economy and Innovation, Quebec Government. The laboratory experiments were carried out in the laboratories of the Center of Excellence in Transportation, Electrification and Energy Storage (CETEES). This work is done in partnership with Fraunhofer R&D Center Electromobility FZEB through a mutual research agreement. Girard Gabriel and Collin-Martin Steve are acknowledged for their contributions in the laboratory experiments.

Conflict of interest

The authors declare no conflict of interest.

Keywords: lithium modification · solid-state batteries · garnet LLZO · interface resistance · silane

- [1] W. Luo, Y. Gong, Y. Zhu, K. K. Fu, J. Dai, S. D. Lacey, C. Wang, B. Liu, X. Han, Y. Mo, E. D. Wachsman, L. Hu, *J. Am. Chem. Soc.* **2016**, *138*, 12258–12262
- [2] A. Mauger, C. Julien, A. Paoella, M. Armand, K. Zaghib, *Mater. Sci. Eng. R* **2018**, *134*, 1–21
- [3] B. Commarieu, A. Paoella, J. C. Daigle, K. Zaghib, *Curr. Opin. Electrochem.* **2018**, *9*, 56–63
- [4] R. Murugan, V. Thangadurai, W. Weppner, *Angew. Chem. Int. Ed. Engl.* **2007**, *4*, 7778–7781
- [5] D. Safanama, D. Damiano, R. P. Rao, S. Adams, *Solid State Ionics* **2014**, *262*, 211–215
- [6] Y. Li, B. Xu, H. Xu, H. Duan, X. Lü, S. Xin, W. Zhou, L. Xue, G. Fu, A. Manthiram, J. B. Goodenough, *Angew. Chem. Int. Ed. Engl.* **2017**, *87545*, 771–774
- [7] C. Ma, Y. Cheng, K. Yin, J. Luo, A. Sharafi, J. Sakamoto, J. Li, K. L. More, N. J. Dudney, M. Chi, *Nano Lett.* **2016**, *16*, 7030–7036
- [8] W. Zhou, S. Wang, Y. Li, S. Xin, A. Manthiram, J. B. Goodenough, *J. Am. Chem. Soc.* **2016**, *138*, 9385–9388
- [9] K. Fu, Y. Gong, B. Liu, Y. Zhu, S. Xu, Y. Yao, W. Luo, C. Wang, S. D. Lacey, J. Dai, Y. Chen, Y. Mo, E. Wachsman, L. Hu, *Sci. Adv.* **2017**, *3*, e1601659
- [10] L. Porcarelli, C. Gerbaldi, F. Bella, J. R. Nair, *Sci. Rep.* **2016**, *6*, 19892
- [11] A. Umeda, E. Menke, M. Richard, K. L. Stamm, F. Wudl, B. Dunn, *J. Mater. Chem.* **2011**, *21*, 1593–1599
- [12] S. Neuhold, J. T. Vaughey, C. Grogger, C. M. López, *J. Power Sources* **2014**, *254*, 241–248
- [13] M. Armand, *Solid State Ionics* **1983**, *9*, 745–754
- [14] M. Nakayama, S. Wada, S. Kurokic, M. Nogami, *Energy Environ. Sci.* **2010**, *3*, 1995–2002
- [15] K. Park, B. C. Yu, J. W. Jung, Y. Li, W. Zhou, H. Gao, S. Son, J. B. Goodenough, *Chem. Mater.* **2016**, *28*, 8051–8059
- [16] W. Luo, Y. Gong, Y. Zhu, Y. Li, Y. Yao, Y. Zhang, K. Fu, G. Pastel, C. F. Lin, Y. Mo, E. D. Wachsman, L. Hu, *Adv. Mater.* **2017**, *29*, 1606042
- [17] C. Wang, Y. Gong, B. Liu, K. Fu, Y. Yao, E. Hitz, Y. Li, J. Dai, S. Xu, W. Luo, E. D. Wachsman, L. Hu, *Nano Lett.* **2017**, *17*, 565–571

- [18] H. Buschmann, J. Dölle, S. Berendts, A. Kuhn, P. Bottke, M. Wilkening, P. Heitjans, A. Senyshyn, H. Ehrenberg, A. Lotnyk, V. Duppel, L. Kienlee, J. Janek, *Phys. Chem. Chem. Phys.* **2011**, *13*, 19378
- [19] H. Ohta, A. Mizutani, K. Sugiura, M. Hirano, H. Hosono, K. Koumoto, *Adv. Mater.* **2006**, *18*, 2226
- [20] A. Sharafi, E. Kazyak, A. L. Davis, S. Yu, T. Thompson, D. J. Siegel, N. P. Dasgupta, J. Sakamoto, *Chem. Mater.* **2017**, *29*, 7961–7968
- [21] L. Cheng, E. J. Crumlin, W. Chen, R. Qiao, H. Hou, S. F. Lux, V. Zorba, R. Russo, R. Kostecki, Z. Liu, K. Persson, W. Yang, J. Cabana, T. Richardson, G. Chen, M. Doeff, *Phys. Chem. Chem. Phys.* **2014**, *16*, 18294–1830
- [22] L. Cheng, W. Chen, M. Kunz, K. Persson, N. Tamura, G. Chen, M. Doeff, *ACS Appl. Mater. Interfaces* **2015**, *7*, 2073–2081
- [23] L. Cheng, J. S. Park, H. Hou, V. Zorba, G. Chen, T. Richardson, J. Cabana, R. Russo, M. Doeff, *J. Mater. Chem. A* **2014**, *2*, 172–181
- [24] H. El Shinawi, J. Janek, *J. Power Sources* **2013**, *225*, 131–139

Manuscript received: January 16, 2019
